REGISTRATION OF HIGH RESOLUTION SAR AND OPTICAL SATELLITE IMAGERY IN URBAN AREAS

S. Suri[a]*, S. Türmer[a,b], P. Reinartz[a], U. Stilla[b]

[a]Remote Sensing Technology Institute (IMF), German Aerospace Center (DLR) PO Box 1116,
D-82230 Wessling, Germany (Sahil.Suri, Peter.Reinartz, Sebastian.Tuermer)@dlr.de
[b] Photogrammetry and Remote Sensing, Technische Universität München (TUM)
Arcisstrasse 21, 80333 Munich, Germany
stilla@tum.de

Commission IV, WG IV/3

ABSTRACT:

With the launch of high resolution remote sensing satellites in different modalities like TerraSAR-X, WorldView-1 and Ikonos, the contribution of remote sensing for various applications has received a tremendous boost. Specifically, the combined analysis of high resolution SAR and optical imagery is of immense importance in monitoring and assessing catastrophes and natural disaster. Although, latest satellites provide georeferenced and orthorectified data products, still registration errors exist within images acquired from different sources. These need to be taken care off through quick automated techniques before the deployment of these data sources for remote sensing applications. Modern satellites like TerraSAR-X and Ikonos have further widened the existing gap of sensor geometry and radiometry between the two sensors. These satellites provide high resolution images generating enormous data volume along with very different image radiometric and geometric properties (especially in urban areas) leading to failure of multimodal similarity metrics like mutual information to detect the correct registration parameters. In this paper we present a processing chain to register high resolution SAR and optical images by combining feature based techniques namely, homogeneous regions extracted from high resolution images and intensity based similarity metrics namely normalized cross correlation and mutual information. Our test dataset consist of images from TerraSAR-X and Ikonos acquired over the city of Sichuan, China. First results from registration show good visual alignment of SAR and the optical image.

1. INTRODUCTION

High resolution remote sensing images are important in various civilian and military applications, like traffic studies, treaty and boarder monitoring, generation of 3D models and topographic maps, urban growth, damage assessment and disaster mitigation. For these tasks, images acquired by both passive and active high resolution spaceborne sensors like Quickbird, Ikonos, and TerraSAR-X have a potential of being utilized to a great effect. All the mentioned sensors here are nearly in the same league of ground sampling distance (GSD), about 1 meter, which is expected to improve further in near future. Specifically, images acquired both by the passive optical sensors and active SAR sensors (alone and in combination) are major sources for crisis information management. The SAR sensor's active nature utilizing microwaves gives them the capability to see through clouds and to acquire images at night which might be the only possible option during a catastrophic event. However, images acquired by SAR sensors have very different characteristics from normally used optical sensor images. On top of the very different geometry (side looking and measuring of distances) from their optical counterparts (measuring angles), images acquired by SAR sensors show a high amount of speckle influence caused by random backscatter of the microwaves emitted by the active sensor. Normally, remote sensing applications might need to accommodate images from different sensors/modalities, depending upon specific application demands or data unavailability. For example, in case of a natural calamity, decision makers might be forced to use an old archived optical data with a newly acquired (post disaster) SAR image. Further, remote sensing imagery acquired at the time of a crisis might have different accuracy levels for example the Ikonos2 standard GEO product (orthorectified without a DEM) might have an accuracy of about 100 meters (Meinel and Reder, 2001) and TerraSAR-X EEC product provides 1 to 4 meter (accuracy tested by corner reflectors in Nonaka et al., 2008). A sample georeferencing difference between two acquired data products during times of emergency can be visualized in Figure 1, where a TerraSAR-X image acquired over the city of Sichuan just after the deadly earthquake on 12/05/08 when overlaid with an old archived pre disaster Ikonos image shows huge registration errors posing problems for any effective application. Combining these two data products for disaster mitigation and using various remote sensing techniques like mapping, change detection, fusion and GIS overlays might not yield fruitful results and therefore image to image registration becomes really important and an absolute necessity. Certain recent efforts in registering urban area images from airborne SAR sensors and optical satellite images like IKONOS have been made by combining feature and intensity based techniques (Lehureau, 2008; Wegner et al., 2008; Oller et al., 2006) and these reflect the lastest in research catering to remote sensing image registration problems. Henceforth, in this paper, we present an automated registration processing chain to accomplish image to image registration especially for high resolution imagery acquired over urban areas. In the following sections, we elaborate our proposed

registration chain, experimental dataset and methodology and finally we discuss the obtained results, draw conclusions and outline our efforts to enhance the processing chain for addressing challenges of the very near future.

2. PROPOSED REGISTRAION CHAIN

Image registration refers to the task of aligning two or more images acquired at different times, from different sensors or from different view points. Image registration can roughly be classified into categories namely, feature based and intensity based techniques. An extensive overview and survey of various image registration methods used in the above mentioned fields can be found in Brown (1992).

Figure 1. GIS overly of a TerraSAR-X and an Ikonos image

For registration of SAR and optical imagery, intensity based techniques have an advantage over the feature based techniques as successful detection and matching of images from these very different sensors is a meticulous task. For intensity based techniques, the problem of registration is generally mapped as an optimization problem. Where the spatial transformation function T is the argument of the optimum of some similarity metric S, applied to reference image I_R and transformed input image I_{TI}. This can be expressed as:

$$T = \arg(opt(S(I_R, I_{TI}))) \qquad (1)$$

The registration chain utilized here for registering high resolution SAR and optical imagery acquired over urban areas, has it roots from the analysis accomplished in Suri and Reinartz (2009). In the cited reference, we highlighted that mutual information (registration similarity metric S in Equation 1) can be very well adapted for registration of SAR and optical high resolution satellite imagery in urban areas. The major conclusion from the cited work was that mutual information did show enough capability of handling very different SAR and optical sensor geometry through segmentation steps introduced only in the SAR image.

Here in this paper, we go a step forward and test the similarity metric capability under operational settings. In general, mutual information based image registration is generally mapped as an optimization problem with an idea of finding a transformation registration function which maximizes MI within the images being registered. Two issues that need to be addressed while handling any optimization problem (here intensity based registration) are the following:

Optimizer selection: A vigilant review of the literature available for intensity based registration algorithms gives us a lot of options to select an optimizer for the presented task. For further reading, Pluim et al. (2003) also presented a survey of optimization techniques utilized in MI based registration. In this paper, the multiresolution approach presented by Cole Rhodes et al., (2003) to register Landsat imagery by maximizing mutual information between the features extracted by Steerable Simoncelli Filters using the SPSA algorithm has been extended for much more general purposes.

Optimizer Initialization: After selecting a suitable optimizer we normally require an initialization to start the entire process of image registration. Normally, this can be done manually by just roughly marking out a point or two in the images being registered. This process though minuscule in size, bears a lot of importance on the overall registration performance. As having an initialization too far from the real registration parameters can cause the optimizer to halt in a spurious peak leading to failure of the registration chain. ´
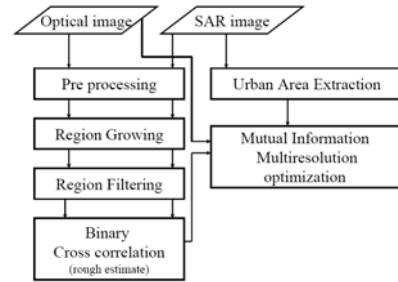

Figure 2. Proposed registration chain

The proposed processing chain has been depicted in Figure 2. It can be visualized that the chain has two distinct components. One component based upon the region growing concept is targeted to estimate rough registration parameters that can be utilized as the seed parameters for the multiresolution mutual information optimization.

All the utilized components of the processing chain would now be discussed with respect to their importance as well as their theoretical and implementation details.

2.1 Estimating Rough Registration Parameters

As already mentioned, the task of estimating the rough registration parameters form an important component of the entire optimization process. In this paper, we attempt to automate this important step by introducing a concept which can also be extended to register much higher resolution SAR and optical urban area images in near future. The main hindrance in a successful registration of high resolution SAR and optical images is the very different sensor geometry that has a significant influence on real world 3D objects. According to the sensor characteristics these 3D real world objects appear very differently in 2D images imaged by both the SAR and optical sensors (Stilla, 2007). The SAR side looking geometry leaves its impact in form of the parallax, shading and double bounce effects in urban areas. Radiometric and geometric differences also become clearly visible, especially on man made objects like bridges might appear very differently in SAR and optical images (Wegner and Soergel, 2008)

Considering the very incompatible information generated by the two sensors in urban areas (especially for 3D objects) the idea here is to select only on ground 2D features (image appearance is not greatly influenced by sensor geometry) for registration purposes. In general, for high resolution satellite images acquired over urban areas, common city features like wide roads, rivers, big stadiums, play grounds, parks can be expected to appear in considerable sizes and be represented by relatively homogeneous intensity values (if imaged without occlusions, especially in the case of SAR sensor). This hypothesis gets confirmed as we analyze the

appearance of prominent features like river and roads in the images depicted in Figure 2. Considering this regular, homogeneous appearance of flat urban features, we intend here to utilize region growing techniques to obtain homogenous features within the images.

To initiate the registration process, some kind of smoothing operation is mandatory before targeted flat homogeneous regions can be extracted for registration purposes. Considering the image statistics, we have employed an enhanced Frost filter (Lopes et al., 1990) for SAR image and the Gaussian filter for optical image smoothing. Following the region extraction using the standard region growing technique (Castleman, 1996), we attempt to filter the obtained homogeneous regions on basis of their shape properties like area, length and geometrical moments. The selection of the desired homogeneous flat regions leads to two binary region images from both the SAR and the optical image. To estimate the registration parameters we then employ normalized cross correlation (NCC) to estimate registration parameters between the two region images. Further, we intend to use these as initialization parameters for multiresolution MI optimization (Cole Rhodes et al., 2003).

2.2 Mutual Information Based Fine Registration

The applicability of mutual information as registration metric for high resolution satellite imagery in urban areas was highlighted in Suri and Reinartz (2009). In the cited reference, we proposed segmentation steps (based on histogram thresholds) in the SAR image and did a through analysis on the interdependence of the segmentation step and mutual information (MI) performance. In this paper, we evolve the earlier proposed segmentation step based upon the SAR image histogram with a more appropriate pre processing technique.

Urban Area Detection

The idea behind this step is to get rid of the pixels generated by real world 3D structures as these pixels are incompatible due to very different sensor geometry and therefore should not be accounted for in similarity metric computation. Urban area extractions from SAR imagery has been researched quite extensively and quiet a few robust techniques based upon local SAR characteristics (Gouinaud and Tupin, 1996) and special textural information (Lorette 1999) have been proposed and successfully utilized. For the presented work we employ the method proposed in Lorette (1999) which is based on simple local variance computation. This method works on the principle that variance around the urban pixels is very high in all the eight directions surrounding it. Therefore, in case the local variance's in eight directions from a center point of a window (user definer parameter) is higher than a threshold value (user defined parameter) the pixel is set to be in the urban category. Further, this technique of urban area detection to save time can also be performed on down sampled images (Oller et al., 2006).

Multiresolution Mutual Information Optimization

MI has evolved from the field of information theory. MI describes a statistical dependence between two random variables (e.g. A and B) expressed in terms of variable entropies. Normally, Shannon entropy (additive in nature) is utilized to represent variable entropies (information content) and for this case MI between two variable A and B is defined as

$$MI(A,B) = H(A) + H(B) - H(A,B) \qquad (2)$$

Above, H(A) and H(B) are the Shannon entropies of A and B respectively, H(A, B) is the joint entropy of B and A. Considering two remote sensing images to be registered as the two random variables, MI is a symmetric relation that always achieves values greater than zero. Registration of two images A and B is based on maximization of MI (A, B) (Equation 2). The marginal entropies and the joint entropy can be computed from the estimated joint histogram according to formulations described in (Chen et al., 2003).

3. DATASET AND METHODOLOGY

As already highlighted in section 1, we present this paper in context of disaster mitigation applications where very fast and robust image to image registration might be needed before utilizing remote sensing techniques on acquired datasets. Our test dataset include TerraSAR-X and Ikonos imagery acquired over the city of Sichuan in China (dataset details in Table 1). The TerraSAR- X image has been acquired three days after the disastrous earthquake on 12-May-2008 and along with it we also have pre and post disaster Ikonos scenes. The Ikonos image here is the standard geometrically corrected scene which is expected to have a planar accuracy of 100m (Meinel and Reder, 2001). The utilized TerraSAR-X image has predicted orbit accuracy and it is the Geocoded Ellipsoid Corrected (GEC) product. GEC products are corrected to UTM projection using the WGS84 ellipsoid with an average terrain height. GEC products are not the best TerraSAR-X products as far as on ground accuracy is concerned but in times of calamity these might be the only available option due to timing constraints and possible unavailability of a DTM.

	TerraSAR-X	Ikonos (pre disaster)	Ikonos (post disaster)
Mode	High Res spot light (HS)	Forward scanning	Reverse Scanning
Spectral Resolution	9.65 GHz	450 - 900 nm	450 – 900 nm
Pixel Size	1m	1m (pan)	1m (pan)
Bit depth	16 bit	11 bit	11 bit
Angle	Inc. Angle 50.80°	Nominal Collection Elevation: 62.09°	Nominal Collection Elevation: 59.26°
Date	15/05/08	14/09/07	28/06/8
Processing Level	GEC product	Standard Product	Standard Product

Table 1. Details of the TerraSAR-X and Ikonos-2 imagery of size 1000 x 1000 pixels

As the available products are not the best available products (absolute accuracy wise), we observe georeferencing difference of around 95m in x direction and 45m in y direction between the TerraSAR-X and the post disaster image. Further, the georeferencing difference between the TerraSAR-X and the pre disaster image is estimated to be around 125m in x direction and 25m in y direction. All the three images selected for the analysis can be visualized can be visualized in Figure 3. It is worthwhile to note that the same standard geometrically corrected Ikonos scenes (pre and post disaster) with the same TerraSAR-X scene have significantly dissimilar georeferencing differences.

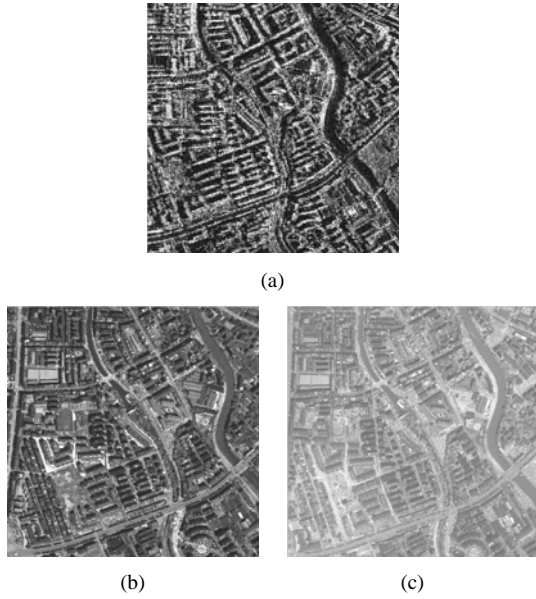(a)

(b)   (c)

Figure 3. Utilized (a) TerraSAR-X (b) Pre disaster Ikonos
(c) Post disaster Ikonos images

As we do not have any ancillary source to evaluate our registration scheme presented in section 2, we perform a consistency analysis using the three images. First, we register both the pre and post disaster Ikonos image to the reference TerraSAR-X image grid bringing both the pre and post disaster Ikonos in the same reference grid. Ideally, any further attempt to register the two transformed Ikonos images on the reference TerraSAR-X grid should yield no misalignment if their individual registrations have been consistent. Therefore, the registration parameters obtained between registered pre and post disaster Ikonos images can give us a fair idea about the similarity metric consistency.

4. RESULT AND DISCUSSION

4.1 Region Extraction

The extracted regions overlaid over the three involved images can be visualized in Figure 4. A vigilant look at the region growing results produced in Figure 4 clearly highlights the huge amount of extracted regions with prominent city roads and rivers as the most significant regions in both the SAR and optical images. Along with these, a lot of building roof tops, sensor geometry effects (layover, shadow) and other city occlusions have also been detected simply because of their quite homogeneous appearance in high resolution imagery.

The idea further would now be to select a subset of these regions whose appearance is independent of the sensor geometries (on ground 2D features). This is a very important step for the entire processing chain as those regions whose image appearance is independent of the sensor geometry can only be utilized for matching purposes, all other remaining regions can be considered as incompatible for the task in hand. To achieve the desired objective we do a region filtering step where we filter regions on basis of their length, area and geometric moments (results in Figure 5).

It is observed that different regions appear in the three images being considered for the analysis. This can be considered as a general scenario that extracting exactly the

same regions in images acquired by different sensors or in different condition might just not be possible. Main objective of this step should be to get a good number of common and sensor geometry independent regions in the images being registered.
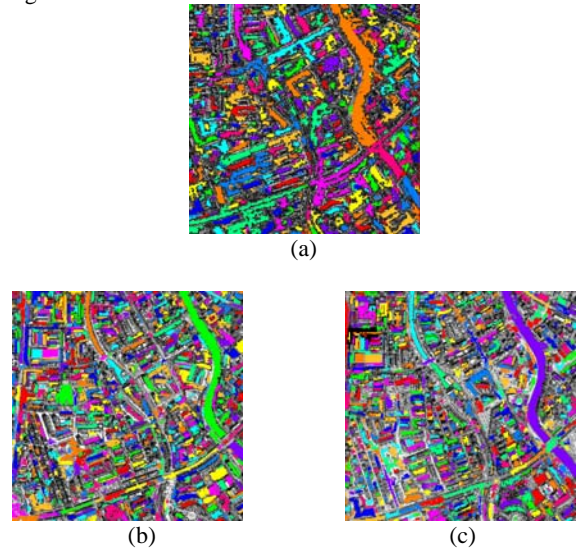

(a)

(b)   (c)

Figure 4. Extracted regions overlaid on (a) TerraSAR-X
(b) Pre disaster Ikonos (c) Post disaster Ikonos images

(a)

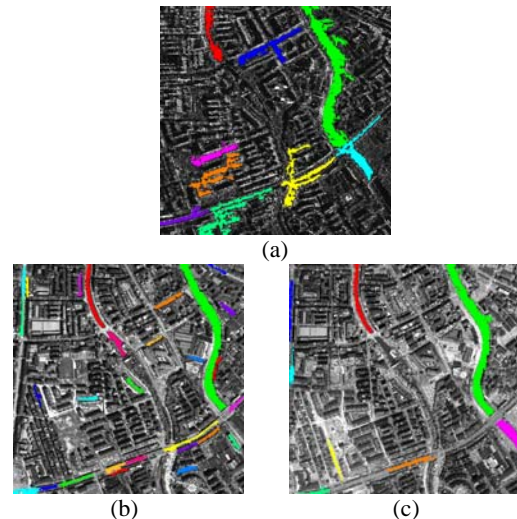(b)   (c)

Figure 5. Filtered regions from (a) TerraSAR-X
(b) Pre disaster Ikonos (c) Post disaster Ikonos images

It is still a possibility to have few undesirable regions like the one in pre disaster Ikonos image (Figure 5b) where we have certain building roof tops and shadows still appearing as regions participating in the final matching process. Considering the fact that it can be a tedious task to get all the desirable regions in the images being registered, the processing chain does require a robust similarity metric to match the extracted regions.

4.2 Region Matching with Binary Cross Correlation

The finally extracted and filtered regions are represented as binary region images. Further, with an assumption that most of the information contained within binary region images can be utilized for estimating the registration parameters, we utilize the normalized cross correlation for the elucidated task. In this case, we obtain a NCC peak between

TerraSAR-X and pre and post disaster Ikonos images at (-120, -27) and (-84, -45) pixel translation in x and y directions respectively.

4.3 Urban Area Detection

To precede the multiresolution MI optimization an urban area step in the SAR image is mandatory to expect any fruitful results from the registration processing chain. The result of binning out the incompatible SAR image pixels using a texture based method can be visualized in Figure 6.
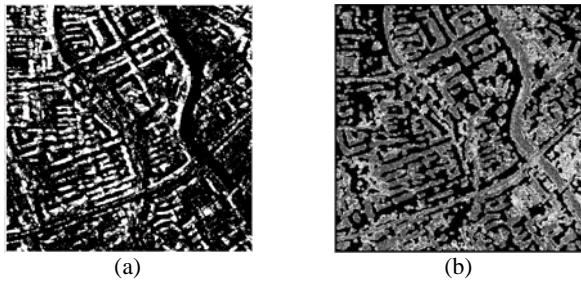

(a)   (b)

Figure 6. (a) Result of urban area detection and morphological closing with disk operator of radius 5 on the TerraSAR-X image (white pixels are the detected urban area pixels).
(b) Segmented TerraSAR-X image

4.4 Multiresolution MI Optimization

To estimate the final registration parameters, we utilize the TerraSAR-X image depicted in Figure 6b as the reference image for the 2 Ikonos images depicted in Figure 3(b, c). The concept here is to down sample the images involved to one forth of their 1m pixel spacing and start optimizing the MI function from the 4m images and then move up the image pyramid successfully to obtain the desired registration results. The results obtained from this registration process along with their registration turn around time can be analyzed in Table 2. The results obtained from NCC process (utilized as a seed for the MI process) have also been tabulated for comparison purposes

SM	Pixel Size	Pre Iko to TSAR-X	Post Iko to TSAR-X	RD	TAT
NCC	1m	(-120, -27)	(-84, 45)	(2,4)	20 Sec
MI	4m	(-129, -27)	(-94, -50)	(3,1)	24 Sec
MI	2m	(-132, -26)	(-94, -50)	(0,2)	60 Sec
MI	1m	(-131, -26)	(-94, -50)	(1,2)	240 Sec

Table 2. Registration results obtained using NCC and MI

In Table 2 we report registration differences (RD) obtained within the transformed pre Ikonos and Post Ikonos images at a particular pixel spacing with the specified similarity metric, ideally this should be 0m in both x and y directions symbolizing exactly the same registration of the pre and post Ikonos images on the TerraSAR-X image grid. RD has been estimated by exhaustively searching the MI peak in a registration search space of [-10 +10] pixels in x and y direction between the transformed pre and post Ikonos images on the reference image grid. TAT refers to the total registration turn around time (Pre Ikonos to TerraSAR-X and Post Ikonos to TerraSAR-X combined) in a parallel execution environment at a particular pixel spacing using the specified similarity metric. As very much expected, the NCC due to its nature produced much lower registration TAT compared to joint histogram based MI (all the experiments have been done on Genuine Intel Pentium D CPU (2.8 GHz) with 2 GB RAM).

The Ikonos images when transformed over the reference TerraSAR-X reference gird using the registration parameters obtained using the NCC metric show registration errors which are then further refined using MI. It can be safely argued that both the similarity metrics performed their assigned tasks as their individual RD statistic is very much closer to the desired value of 0m in both X and Y directions, signifying a consistent registration performance. Readers are advised to be cautious while interpreting the RD statistic as it is mere a similarity metric consistency measure and the values obtained have no relation with the quality of registration achieved. The parameters obtained using MI show better alignment within the image features but without any ancillary information an absolute accuracy evaluation of the obtained parameters is just not possible. It can also be observed that there is not very significant difference (keeping registration TAT in perspective) between the registration parameters obtained at 4m pixel spacing and at 1m pixel spacing while utilizing MI as the similarity metric. The pre disaster Ikonos image registered with the reference TerraSAR-X image using the parameters obtained by MI at pixel spacing 1m can be visualized in Figure 7.

Figure 7. Registered TerraSAR-X and Ikonos image

5.0 CONCLUSIONS

Automatic image to image registration for high resolution SAR and optical imagery becomes a challenging problem due to the very different sensor geometries which play a dominant role especially in the urban areas. In this paper, we have presented a hybrid solution to high resolution SAR optical image registration problem by combining the concept of feature based (2D homogenous regions) and intensity based (NCC and MI) techniques to solve the coveted problem. The processing chain tested on various other datasets (different satellite sensors, scene area) has shown similar performance. We would like to report that other subsets from the same complete scenes utilized in this registration exercise yielded different registration parameters signifying the presence of local deformation within the complete scenes (both optical-SAR and optical-optical). The foremost challenge here is to find out the exact registration parameters which without any ancillary

information look a tedious task. Due to the very nature of high resolution SAR and optical imagery, registration assessment becomes highly subjective to visual assessment making evaluation a tough ask. In our future plans we intend to test the developed processing chain rigorously on various datasets and also aim to do a through analysis about the accuracy of the achieved registration parameters. In general, we expect better registration in the azimuth direction but due the layover and shadow influence dominant in the range direction we expect the true registration parameter to be within a range of 5m. Further, the following can be concluded about the utilized tools in the presented registration chain:

We have utilized the technique of region growing to extract the 2D on ground features in both the SAR and the optical imagery. Region growing seems to be a promising technique especially for high resolution imagery where lot of features of interest for image to image registration having homogeneous appearances. As already highlighted region growing technique may face problems of roof tops, sensor geometric influence and city occlusions being detected and these might hinder the registration chain performance.

Normalized cross correlation with its extremely fast capability to estimate shifts within the binary region images has good potential for being utilized for registration of high resolution images. In general the results obtained from NCC have not been found to be very accurate (visually). It is very likely that conjugate regions in images acquired under different conditions and/or by different sensors may not be extracted in exact shapes and sizes posing problems for NCC to estimate accurate registration parameters. Anyhow, as demonstrated, these can be successfully utilized to initialize a MI based registration process yielding better registration results.

The urban area extraction (predominantly removes very bright pixels generated due to double and triple bounce effect) is mandatory for successful application of MI for high resolution SAR and optical images. It has already been highlighted that MI offers robust registration performance for different levels of image segmentation (Suri and Reinartz, 2009) therefore the performed urban area extraction is not foreseen as a very critical step of the registration chain. In future applications, to completely automate the entire processing chain, we aim to develop individual components which are not very sensitive to parameter settings and this urban area extraction step certainly seems to fit in the desired requirements.

MI lies at the heart of the entire processing chain, the capability of MI to handle SAR and optical image radiometry for image registration has been exploited to develop the proposed registration chain. The capability of MI to estimate quite accurate registration parameters from down sampled imagery can very well be utilized to expedite the registration process considerably.

REFERENCES

Brown, L.G., 1992. A survey of image registration techniques, *ACM Computing Surveys*, 24 (4), pp. 325-376.

Castleman, K. R., 1996. *Digital Image Processing*, Prentice Hall.

Chen, H., Varshney, P.K., and Arora, M.K., 2003. MI based image registration for remote sensing data. *International Journal of Remote Sensing,* 24(18), pp. 3701-3706.

Cole Rhodes, A.A., Johnson, K.L., LeMoigne, J., and Zavorin, I., 2003a. Multiresolution registration of remote sensing imagery by optimization of mutual information using a stochastic gradient, *IEEE Transactions on Image Processing*, 12 (12), pp. 1495-1511.

Gouninaud, F., and Tupin, F., 1996. Potential and use of radar images for characterization and detection of urban areas. *In Proc: IEEE Geoscience and Remote Sensing Symposium*, 1, pp. 474-476, Lincoln, NE, May 1996.

Lehureau, G., Tupin, F., Tison, C., Oller, G., and Petit, D., 2008. Registration of metric resolution SAR and optical images in urban areas, *In Proc. 7th European Conference on Synthetic Aperture Radar*, Friedrichshafen, Germany, June 2008.

Lopes, A., Touzi, R., and Nezry, E., 1990. Adaptive Speckle Filters and Scene Heterogeneity, *IEEE Transactions on Geoscience and Remote Sensing*, 28 (6), pp. 992-1000.

Lorette, A., 1999. Texture analysis through Markov random fields: urban area extractions. *In Proc: IEEE International Conference on Image Processing (ICIP)*, Kobe, Japan, October 1999.

Meinel, G., and Reder, J., 2001. Ikonos Satellitenbilddaten - Ein erster Erfahrungsbericht, *Kartographische Nachrichten, Kirschbaumverlag*, 1, pp. 40-46 (in German).

Nonaka, T., Ishizuka, Y., Yamane, N., Shibayama, T., Takagishi, S., and Sasagawa, T., 2008. Evaluation of the Geometric Accuracy of TerraSAR-X, *In Proc: 21st ISPRS Congress*, Beijing, China, July 2008.

Oller, G., Petit, D., and Inglada, J. 2006. On the use of SAR and optical images combination for scene interpretation, *ISPRS Symposium, Commission I, WGI/3, From Sensors to Imagery*, 2006.

Pluim, J., Maintz, J., Viergever, M., 2003. Mutual information based registration of medical images: a survey, *IEEE Transactions on Medical Imaging*, 22(8), pp. 986-1004.

Stilla, U., 2007. High resolution radar imaging of urban areas, *In: Fritsch D (ed) Photogrammetric Week, 2007*, Wichmann, pp. 149-158, Stuttgart, Germany.

Suri. S., and Reinartz, P., 2009. On the Possibility of Intensity Based Registration for Metric Resolution SAR and Optical Imagery, *In Proc: 12th AGILE International Conference on Geographic Information Science*, Hannover Germany, June 2009.

Wegner, J.D., Inglada, J., and Tison, C., 2008. Automatic fusion of SAR and optical imagery based on Line Features, *In Proc. 7th European Conference on Synthetic Aperture Radar*, Friedrichshafen, Germany, June 2008.

Wegner, J.D., and Soergel, U., 2008. Registration of SAR and optical images containing Bridges over land, *In Proc: EARSel Workshop Remote Sensing - New Challenges of High Resolution*, Bochum, Germany, March 2008.